RESEARCH

20 W, 15 ns High-repetition-rate and high-beam-quality MOPA laser by spherical aberration self-compensation at 1342 nm

Zhibin Ye[1] · Xiaoran Li[1] · Shu Jiang[1] · Fei Wu[1] · Meng Huang[1] · Hanmin Hu[1] · Yunxuan Qi[2,3] · Bin Liu[4] · Hengfeng Yan[5]

Abstract

A master oscillator power amplifier (MOPA) pulsed laser operating at 1342 nm is demonstrated. It consists of an acousto-optical (A-O) Q-switched oscillator and two-stage Nd: YVO$_4$ power amplifiers. The spherical aberration self-compensation technique is used in the second stage amplifier to obtain high-beam-quality laser output. The maximum average output power of 20.4 W is obtained with the oscillator power of 2.0 W and the total pump light power of 184.08 W, corresponding to an optical-optical efficiency of 11.08%. The repetition rate and pulse width are 100 kHz and 14.8 ns, respectively. The beam quality factor is $M_x^2=1.45$ and $M_y^2=1.34$. According to our knowledge, this is the maximum output power with a pulse width of ten-nanoseconds level and repetition rate of one-hundred-kilohertz level by an A-O Q-switch at the wavelength of 1342 nm.

1 Introduction

The high-power nanosecond laser at 1342 nm possessing high-repetition-rate and high-beam-quality has extensive applications in semiconductor manufacturing, frequency conversion, and scientific research [1–4]. Compared to the 1064 nm laser, the 1342 nm laser has a ten times higher absorption in water and a one-third extinction in blood, making it the perfect laser source for surgical procedures. The pulsed laser at 1342 nm is normally used to generate red and blue lasers by nonlinear optical frequency conversion. Many applications of the 1342 nm laser, especially silicon material processing, benefit much from a nanosecond pulse with high power, high-repetition-rate, and high-beam-quality.

Active Q-switching is a typical technique for producing high-repetition-rate pulsed lasers. Ma et al. showed a Q-switched active electro-optical pulsed laser with a minimum pulse width of 2.4 ns, a maximum repetition rate of 100 kHz, and a maximum average output power of 2.42 W [5]. The maximum average output power of 3.2 W was achieved at the pulse repetition frequency (PRF) of 10 kHz and the pulse width of 4.7 ± 0.1 ns for the PRF from 2 to 10 kHz [6]. Zhao et al. presented an average output power of 2.64 W acousto-optical (A-O) Q-switched Nd: YVO$_4$ laser with a PRF range of 5–40 kHz [7]. A high-power high-repetition-rate acousto-optically Q-switched 1342 nm laser was presented with an average output power of 11.2 W and pulse width of 60 ns at a repetition rate of 50 kHz [8]. Compared with the electro-optical Q-switch, the A-O Q-switch does not require a high-voltage driver and has no piezoelectric ring effect under a high repetition rate. However, the pulse width is generally in tens or hundreds of nanoseconds, which is difficult to be narrowed especially at a high repetition rate (such as 100 kHz). The average power is only several milliwatts to several watts. In addition, with the

✉ Zhibin Ye
  nibihzey@zju.edu.cn

✉ Shu Jiang
  retcheywcs@aliyun.com

1 College of Electrical and Information Engineering, Quzhou University, Quzhou 324000, China

2 Megapeak(Suzhou) LASER Technology Corporation Limited, Suzhou 215200, China

3 School of Information Science and Engineering, Shandong University, Qingdao 266200, China

4 Hangzhou Bochang Photoelectric Technology Corporation Limited, Hangzhou 310018, China

5 Changzhou Inno Laser Technology Corporation Limited, Changzhou 21364, China

further increment of the average power, the beam quality will deteriorate.

In this letter, we demonstrate a high power, short-pulse-width, high-repetition-rate, and high-beam-quality master oscillator power amplifier (MOPA) laser at 1342 nm. The A-O Q-switched oscillator is designed to generate a high-repetition-rate and short-pulse-width laser, and the amplifiers are used to obtain high power and manage the beam quality. An average output power of 20.4 W is obtained with an oscillator power of 2.0 W. The repetition rate is 100 kHz with the pulse width of 14.8 ns, and the laser beam quality factor of $M_x^2=1.45$ and $M_y^2=1.34$.

2 Experimental setup and design

The experimental setup is illustrated in Fig. 1. It consists of an A-O Q-switched oscillator and two-stage double-pass Nd: YVO$_4$ power amplifiers. In the oscillator, a fiber-coupled diode laser (LD 1) is used for pumping with a central wavelength of 808 nm and a maximum output power of 10 W with a diameter of 200 μm in CW mode (from nLIGHT, Inc.). Using a 1:1 coupler system (Coupler 1), the pump light is focused into the laser crystal with a spot radius of 100 μm. The a-cut 0.3 at% Nd-ion concentration Nd: YVO$_4$ (3 mm×3 mm×8 mm) is thermally bonded with a YVO$_4$ end cap (3 mm×3 mm×2 mm) (from CASTECH Inc.) which can suppress the thermally induced aberrations. Both end surfaces of the laser crystal are anti-reflection
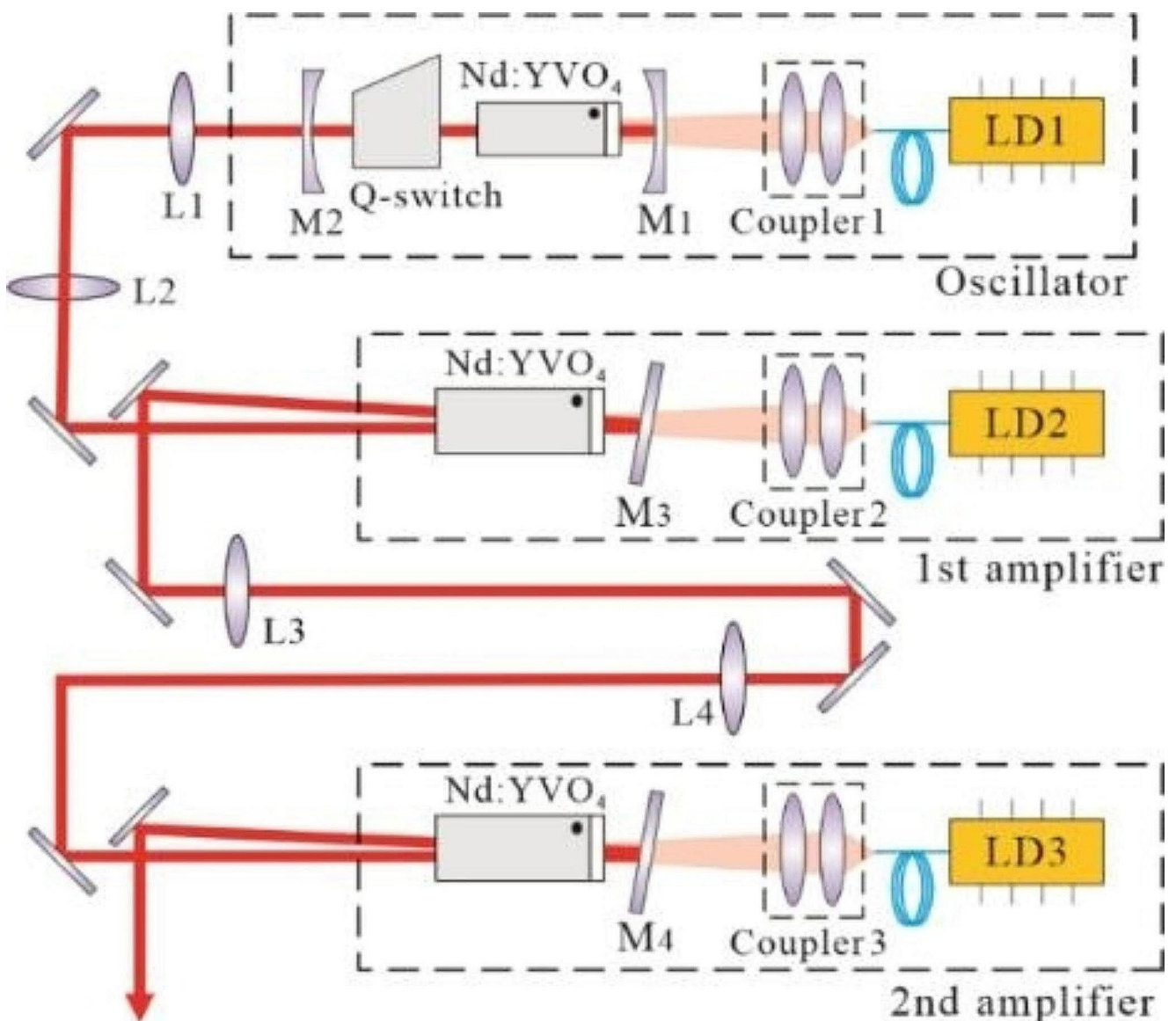

Fig. 1 Experimental setup for 1342 nm MOPA system

(AR) coated at 808 nm, 1342 nm and 1064 nm (to ensure the radiation of 1064 nm would not oscillate). M1 is a rear mirror with a curvature radius of 100 mm. Its flat face is coated in high-transmission (HT) at 808 nm and 1064 nm, while its concave face is coated in high-reflection (HR) at 1342 m and HT at 808 nm and 1064 nm. The output coupler mirror M2 is concave with a curvature of 75 mm and the transmission (T) at 1342 nm is 18%. A 1342 nm A-O Q-switch is inserted between the output mirror M2 and the laser crystal.

The gain should be high enough in the cavity to obtain a narrow-width pulse in the oscillator. The physical cavity length (40 mm) is designed to be as short as possible, and the radius of the pump light in the crystal is designed to be only 100 μm. Furthermore, to lower the pulse rise time, the laser beam radius on the A-O crystal should be small enough, but the laser divergence angle should not be too large, which would limit the diffraction efficiency. A simulation of the laser reproducing-itself (TEM$_{00}$, i.e., ideal Gaussian beam) radius distribution in the cavity is shown in Fig. 2. The crystal's length in the simulation is the same as that in the experiment, consisting of 2 mm of YVO$_4$ and 8 mm of Nd: YVO$_4$. The crystal (thermal effect) is considered to be a perfect thermal lens with the focal length of 90 mm (measured by using a HeNe laser beam to pass through the crystal, the distance between the crystal and the focus of HeNe laser) acting at the bonding surface (dashed line in Fig. 2) and a refractive index of (2.1) The Q-switch crystal is 16 mm long and has a refractive index of (2.2) As the simulation results show, the beam radius on the left and right sides of the Q-switch crystal is only around 87.6 μm, and the divergence angle is just about 0.1 mrad. Thus, the transit time of the acoustic wave across the laser beam decreases and the pulse width is reduced effectively.

After the oscillator, the two-stage double-pass amplifiers are used, as shown in Fig. 1. Both amplifiers have the same structure. The fiber-coupled diode lasers (LD 2 and LD 3) are used for pumping with the central wavelength of 808 nm and a maximum output power of 100 W in CW mode. With the coupler systems (Coupler 2 and Coupler 3), the pump lights are focused into the laser crystals and can be adjusted to different sizes. The a-cut 0.3 at% Nd-ion concentration Nd: YVO$_4$ (3 mm×3 mm×20 mm) is thermally bonded with a YVO$_4$ end cap (3 mm×3 mm×2 mm). Both end sides of the crystals are AR coated at 808 nm, 1342 nm and 1064 nm. Figure 3 depicts the beam radius versus propagation distance in the amplifiers. The oscillator's beam with a radius of 92 μm on the M1 is projected into the Nd: YVO$_4$ (Crystal 1) with a magnification of 2.5 by lenses L1 and L2 with a focal length of 100 mm and 250 mm, respectively. The distance between L1 and L2 is 350 mm. The laser beam radius is 230 μm in the Nd: YVO$_4$. As mentioned in Ref. [9], the output beam quality quickly degrades due to the severe heating effect caused by the focused pump if the pump beam radius in the amplifier is set too low. If the pump beam radius is too large, the gain intensity decreases, which weakens the gain guiding effect and decreases beam quality. The optimum pump beam radius in the Nd: YVO$_4$ is 210 μm which is about 0.9 times of laser beam radius. After the laser beam passes through the first amplifier, the beam is then reflected by the mirror (M3) and goes back into the amplifier again. The M3 is placed as close as possible to Crystal 1 and is HT coated at 808 nm and HR coated at 1342 nm.

The spherical aberration self-compensation technique is used in the second stage amplifier to obtain high-beam-quality laser output [10–13]. The design is as follows (as shown in Fig. 3): The Crystal 1 is at the position of 700 mm. The crystal has a positive spherical aberration after being heavily pumped, so the laser beam has a positive spherical aberration after passing through Crystal 1 at the position of 700 mm. The beam first converges after Crystal 1 and then

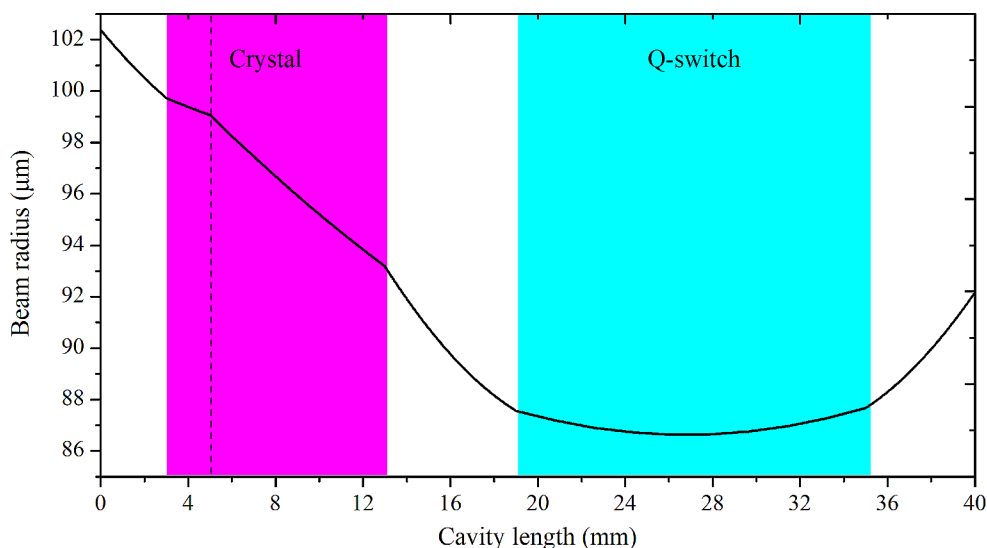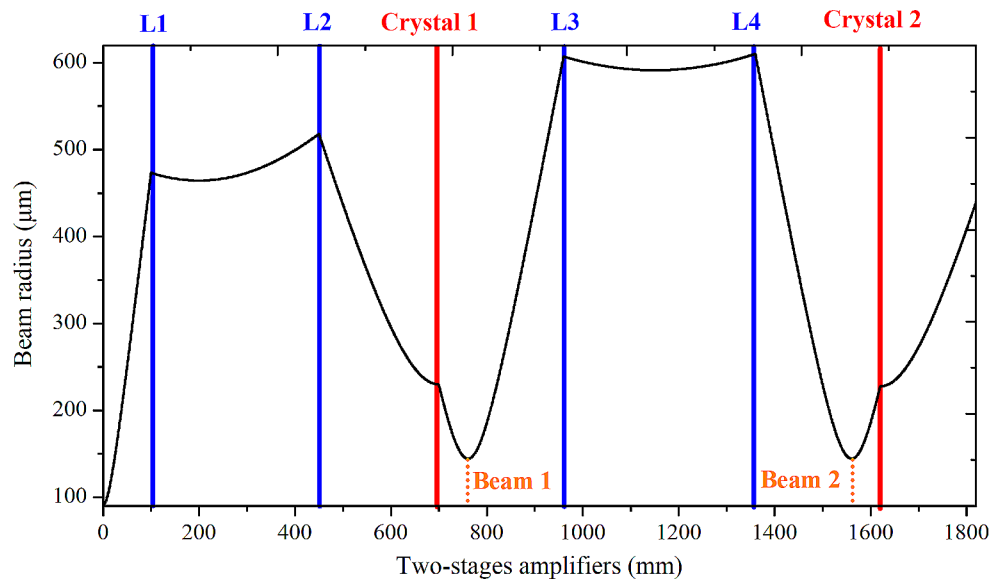Fig. 2 The calculated beam radius distribution in the oscillator

Fig. 3 The beam radius distribution in the two amplifiers

begins to diverge after passing through 760 mm. At the position of 820 mm, the beam size is basically the same as that at 700 mm (after Crystal 1), while the spherical aberration coefficient changes its sign, i.e., from a positive sign to a negative sign, however, the absolute value is basically the same [14, 15]. The two lenses, L3 and L4 (both with a focal length of 200 mm) consist of a 4 F imaging lens system and image Beam 1 to Beam 2 at a 1:1 imaging ratio (IR), as shown in Fig. 3. Thus the beam at the position of 1560 mm is identical to that at 760 mm, and the beam at the position of 1620 mm (60 mm after 1560 mm) is identical to that at 820 mm (60 mm after 760 mm). Therefore, the beam at the position of 1620 mm (before Crystal 2) has a negative spherical aberration coefficient which is basically the same as that of the crystal itself (the absolute value is the same, but the sign is the opposite). Applying Crystal 2's positive spherical aberration coefficient, the negative spherical aberration coefficient is offset after the beam passes through Crystal 2 at the position of 1620 mm, and the beam quality is improved. The experimental results of the beam quality measurements will be shown in the next section.

3 Experimental results and theoretical analysis

The 1342 nm A-O Q-switched oscillator experiment is carried out. With various PRFs, Fig. 4 displays the average output power as a function of absorbed pump power. The output power increases linearly with the increase of absorbed pumping power under 7.13 W. The output power at high PRF is significantly more than that of low PRF at a high pump level. It drops down quickly after peaking at a high pump power of 7.13 W at high repetition frequencies of 40–100 kHz. The

maximum output power value could be maintained in the 7.13–7.98 W pump power at low PRFs of 20 kHz. These are mostly explained by the intense heat effects on the laser crystal and Q-switch, which result in the cavity being unstable and a sharp drop in output power. The highest output power is 2.0 W with a repetition frequency of 100 kHz and an absorbed pump power of 6.28 W, achieving an optical conversion efficiency of 31.8% and a slope efficiency of 33.7%. The pulse widths are 5.1 ns, 6.0 ns, 7.4 ns, 9.8 ns, 15.9 ns with the repetition frequencies of 20 kHz, 40 kHz, 60 kHz, 80 kHz, and 100 kHz, respectively, with the absorbed pump power of 6.28 W, as shown in Table 1 (t_{exp}).

$$t_{cal} = \frac{2L/c}{1 - \ln(r_1) - \xi} \frac{n_0 - n_f}{n_0 - n_{th}[1 + \ln(n_0/n_f)]} \qquad (1)$$

where c is the speed of light, L is the cavity length, $n_0 = K\tau P_p(1 - e^{-1/f\tau})$, f is the PRF, P_p is the pump power, and τ is the fluorescent lifespan. The formula $K = \eta n_{th}/\tau P_{th}$, where P_{th} is the threshold pump power, η is the absorption efficiency, and n_{th} is the threshold inversion density, is obtained using the equation [16]: $n_{th} = \frac{1}{\sigma}[\frac{1}{l}\ln(\xi\sqrt{r_1 r_2})^{-1} + \beta]$, where σ is the stimulated emission cross-section, which can be calculated using Ref. [17], l is the laser crystal's length, ξ is the single pass transmission, r_1 and r_2 are the the M1's and M2's reflectances, and β is the laser crystal's loss coefficient. The relation: $n_f = n_0 e^{-n_0 l\sigma/\gamma}$ can be used to calculate n_f, where $\gamma = 1 - \xi\sqrt{r_1 r_2}e^{-\beta l}$ is a cavity loss factor. The parameters used in the theoretical calculations in Table 2 can be used to determine the output single pulse width at various repetition rates. The results are given in Table 1(n_0, n_f, t_{cal}).

Experimental results are generally consistent with theoretical calculations, which show that the cavity design for

Fig. 4 The oscillator's average output power in relation to absorbed pump power
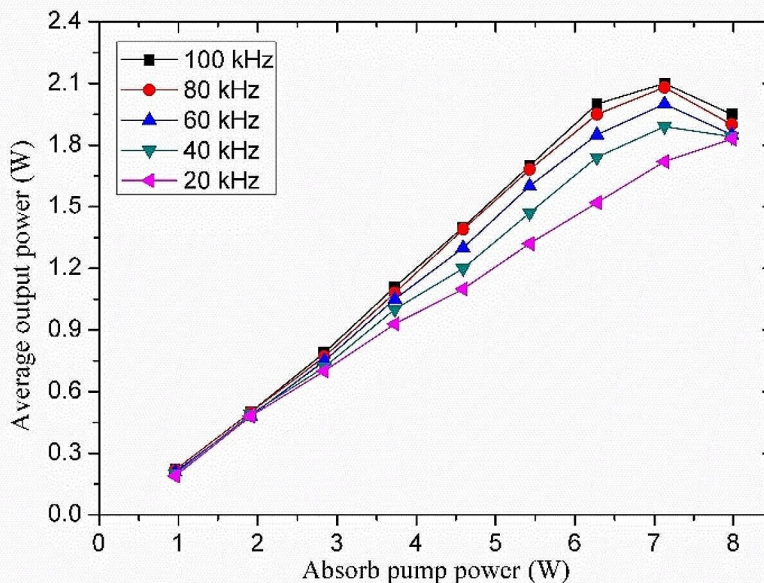

Table 1 The theoretical values and experimental results of the pulse width with different PRFs

PRF (kHz)	20	40	60	80	100
n_0 (cm^{-3})	6.8×10^{18}	3.8×10^{18}	2.6×10^{18}	2.0×10^{18}	1.6×10^{18}
n_f (cm^{-3})	7.4×10^{15}	8.5×10^{16}	1.9×10^{17}	2.7×10^{17}	3.2×10^{17}
t_{cal} (ns)	2.2	3.3	5.0	8.0	14.8
t_{exp} (ns)	5.1	6.0	7.4	9.8	15.9

The pulse width can be expressed as follows [7]

Table 2 Parameters used in theoretical pulse width calculations

τ	110 µs
c	3.0×10^{10} cm/s
η	0.92
P_{th}	0.36 W
σ	1.59×10^{-19} cm^2
l	0.8 cm
ζ	0.98
r_1	1
r_2	0.82
β	0.02 cm^{-1}
L	4 cm
P_p	6.83 W

A-O Q-switching is sensible and optimal. The calculation's presumption that inversion and photon density would remain constant across the laser crystal's transverse section could be the cause of the difference. It restricts the precision with which pulse width and pulse formative time are calculated [16, 18].

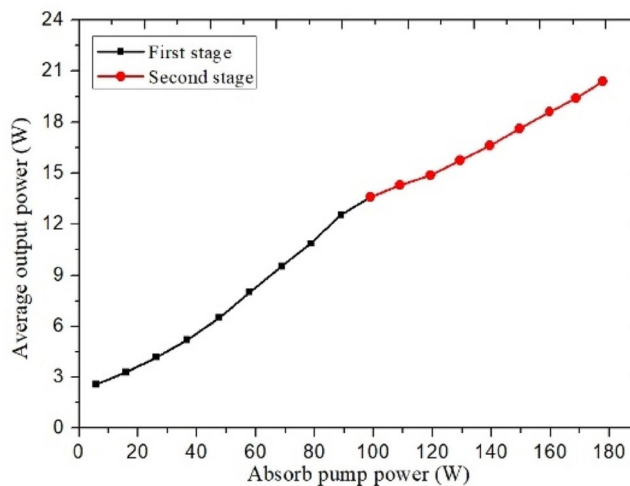The oscillator laser then goes into the two power amplifiers with an average power of 2.0 W, a PRF of 100 kHz,

Fig. 5 The two-stage amplifiers' average output power to absorbed pump power

a pulse width of 15.9 ns, and a beam quality factor of $M_x^2 = 1.05$ and $M_y^2 = 1.08$. Figure 5 depicts the relationship between the two-stage Nd: YVO$_4$ amplifiers' output power and the total absorb LD pump power. With the absorbed pump power in each stage of 88.9 W, the output power of 12.55 W and 20.40 W are achieved from the first and second amplifiers with the optical extraction efficiency of 11.87% and 8.83%, respectively. Because of the diffraction loss, depolarized loss, and absorption loss caused by the Nd: YVO$_4$ rod and mirrors, the slope of the output power of the second-stage amplifier has dropped when compared to the first-stage amplifier. The total optical gain of the two-stage power amplifiers is 10.2.
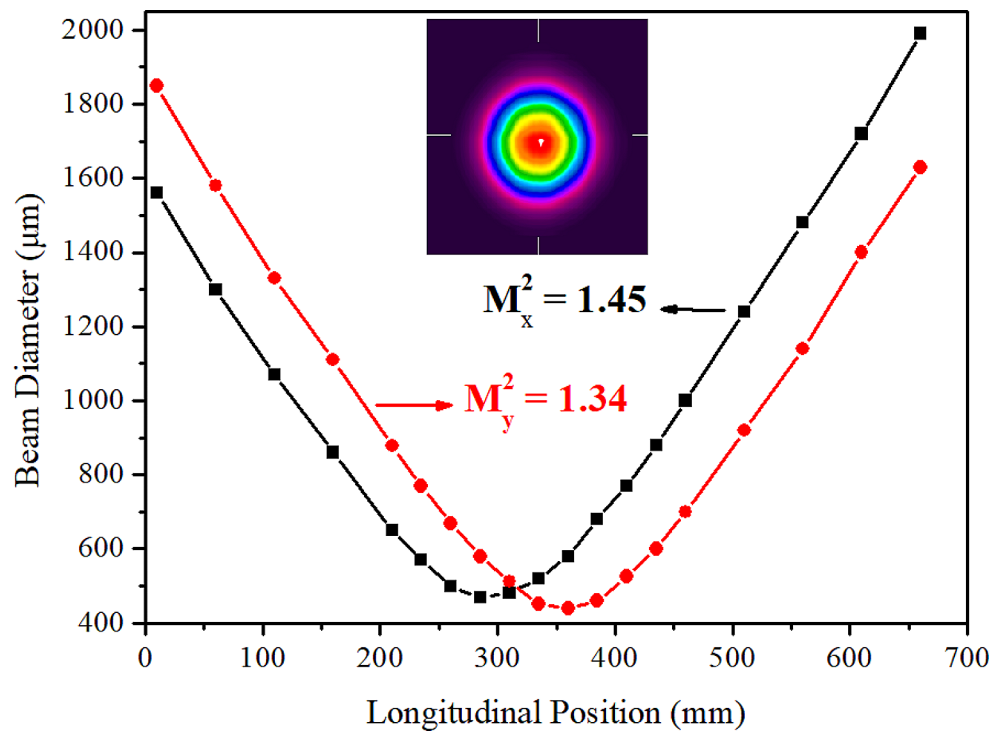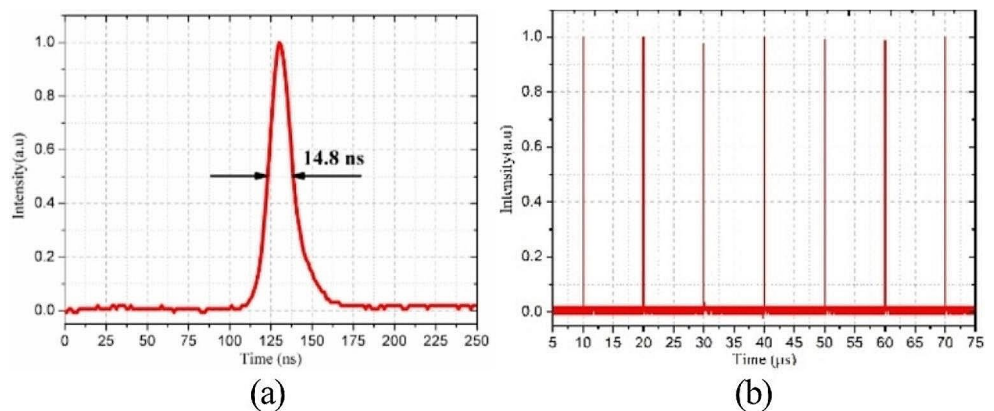
Fig. 6 The measured beam quality M^2 factor

Fig. 7 (**a**) The measured beam single pulse distribution and (**b**) multipulse distribution

The mathematical description of the beam quality factor M^2 for the wavefront aberrations and beam intensity distributions separately [19, 20],

$$M^2 = \sqrt{\left(M^2_{diff}\right)^2 + (M^2_{ab})^2}$$

where M^2_{ab} is the phase term and M^2_{diff} is the amplitude term. Spherical aberration is the dominant factor affecting the beam quality (M^2_{ab}). The laser beam is close to Gaussian intensity distribution at the locations of 700 mm and 1620 mm, i.e., the M^2_{diff} term is close to 1. The variation of the spherical aberration coefficient becomes the main part in changing the beam quality. Thus, as mentioned above, the beam quality deteriorates after 700 mm (Crystal 1) and improves after 1620 mm (Crystal 2). Due to Crystal 1's positive spherical aberration,

the oscillator's beam quality degrades after goes through the first amplifier, and the measurement of the beam quality factor is M$_x^2$=1.91 and M$_y^2$=1.85. Beam quality deterioration is mainly caused by spherical aberration. The beam with negative spherical aberration is compensated by Crystal 2 with positive spherical aberration after passing through the second amplifier, considerably reducing the spherical aberration and enhancing the beam quality. As shown in Fig. 6, the final beam quality factor is decreased with M$_x^2$=1.45 and M$_y^2$=1.34.

As shown in Fig. 7(a), the laser pulse width is measured to be about 14.8 ns. After the two-stage amplifiers, the final pulse of the output laser is very smooth. Compared to the oscillator, the pulse width is slightly narrower, but the gain narrowing effect [21] is minimal. The main reason is that the pulse width of the laser does not reach the femtosecond order. Figure 7(b) shows the output laser multipulse

distribution. The repetition rate is 100 kHz. Each pulse has the same shape and is relatively stable.

4 Conclusions

In this letter, a high-power, high-beam-quality, narrow-width pulse 1342 nm MOPA is reported. In order to obtain a narrow-width pulse, the gain is increased in the oscillator cavity. The divergence angle is designed only 0.1 mrad in the Q-switched crystal to improve the diffraction efficiency. The experimentally measured pulse widths are in general agreement with the theoretically calculated results. The amplifier adopts a two-stage double-pass structure, and in order to prevent the deterioration of the beam quality, the spherical aberration self-compensation technology is adopted. Experimentally, the beam quality is improved while the power is amplified in the second stage amplifier. Finally, a maximum average output power of 20.40 W is obtained with a total pump power of 184.08 W, corresponding to an optical-optical efficiency of 11.08%. The repetition rate and pulse width are 100 kHz and 14.8 ns, respectively. The beam quality factor M^2 is measured to be $M_x^2 = 1.45$ and $M_y^2 = 1.34$. To our best knowledge, this is the highest output power with a pulse width of ten-nanoseconds level and a repetition rate of one-hundred-kilohertz level by an A-O Q-switch at the wavelength of 1342 nm.

Declarations

Competing interests The authors declare no competing interests.

References

1. W.H. Teh, D.S. Boning, R.E. Welsch, Multi-strata stealth dicing before grinding for singulation-defects elimination and die strength enhancement: experiment and simulation[J]. IEEE Trans. Semicond. Manuf. **28**(3), 408–423 (2015)
2. H.C. Liang, F.L. Chang, T.W. Wu et al., Generation of orthogonally polarized mode-locked lasers at wavelength of 1342 nm[J]. IEEE Photonics J. **9**(5), 1–8 (2017)
3. A.M. Rodin, M. Grishin, N. Ulevicius et al., *Picosecond 1342 nm Nd:YVO₄ Laser with 10 W Output at 300 kHz and Conversion to 671, 447, 224 and 192 nm[C]//Advanced Solid State Lasers* (Optica Publishing Group, 2015)
4. Z. Chu, H. Zhang, Y. Wu et al., Passively Q-switched laser based on gold nanobipyramids as saturable absorbers in the 1.3 μm region[J]. Opt. Commun. **406**, 209–213 (2018)
5. S. Ma, D. Lu, H. Yu et al., High repetition rates optically active langasite electro-optically Q-switched laser at 1.34 μm[J]. Opt. Express. **25**(20), 24007–24014 (2017)
6. K. Liu, Y. Chen, F. Li et al., High peak power 4.7 ns electro-optic cavity dumped TEM 00 1342-nm nd:YVO₄ laser[J]. Appl. Opt. **54**(4), 717–720 (2015)
7. Y. Zhao, Z. Wang, H. Yu et al., 6.5-ns actively Q-switched nd:YVO₄ laser operating at 1.34 μm[J]. Chin. Opt. Lett. **9**(8), 081401–081401 (2011)
8. C. Lu, M. Gong, L. Huang et al., High-power high-repetition-rate acousto-optically Q-switched 1342 nm laser[J]. Appl. Phys. B **89**, 285–289 (2007)
9. Z. Xiang, D. Wang, S. Pan et al., Beam quality improvement by gain guiding effect in end-pumped Nd:YVO₄ laser amplifiers[J]. Optics Express **19**(21), 21060–21073 10–15 (2011)
10. H. Qiao, K. Zhong, F. Li et al., Near-diffraction-limit 1-kHz sub-nanosecond diode-end-pumped nd:YAG laser amplifier via self-compensating spherical aberration[J]. Opt. Laser Technol. **164**, 109486 (2023)
11. Y. Qi, Z. Zhao, C. Liu et al., Beam quality management in multi-stage side-pumped nd:YAG MOPA laser systems[J]. IEEE J. Sel. Top. Quantum Electron. **21**(1), 220–225 (2014)
12. Z. Ye, Z. Zhao, S. Pan et al., Beam profile evolution and beam quality changes inside a diode-end-pumped laser oscillator[J]. IEE J. Quantum Electron. **50**(2), 62–67 (2013)
13. C. Feng, S. Chen, L.H. Huang et al., Study on the dynamic control of spherical aberration on the stable zone of the first three low-order modes of LD end-pumped lasers[J]. Opt. Commun. **478**, 126397 (2021)
14. B. Liu, C. Liu, L. Shen et al., Beam quality management by periodic reproduction of wavefront aberrations in end-pumped nd:YVO₄ laser amplifiers[J]. Opt. Express. **24**(8), 8988–8996 (2016)
15. Z. Ye, Y. Wang, Z. Zhao et al., Method to improve beam quality by compensating spherical aberrations in master oscillator power amplifier laser systems[J]. Appl. Opt. **53**(33), 7963–7967 (2014)
16. G. Baldwin, Output power calculations for a continuously pumped Q-switched YAG:Nd^{+3} laser[J]. IEE J. Quantum Electron. **7**(6), 220–224 (1971)
17. N. Mermilliod, R. Romero, I. Chartier et al., Performance of various diode-pumped nd: laser materials: influence of inhomogeneous broadening[J]. IEE J. Quantum Electron. **28**(4), 1179–1187 (1992)
18. J. Liu, C. Wang, C. Du et al., High-power actively Q-switched nd:GdVO₄ laser end-pumped by a fiber-coupled diode-laser array[J]. Opt. Commun. **188**(1–4), 155–162 (2001)
19. B.J. Neubert, B. Eppich, Influences on the beam propagation ratio M^2[J]. Opt. Commun. **250**(4–6), 241–251 (2005)
20. M.L. Gong, Y. Qiu, L. Huang et al., Beam quality improvement by joint compensation of amplitude and phase[J]. Opt. Lett. **38**(7), 1101–1103 (2013)
21. L.W. Casperson, A. Yariv, Spectral narrowing in high-gain lasers[J]. IEE J. Quantum Electron. **8**(2), 80–85 (1972)